Area of Mangrove Forests Calculated by Color Image Segmentation Using k-Means Clustering and Region Growing

by R. Rizal Isnanto

Area of Mangrove Forests Calculated by Color Image Segmentation Using *k*-Means Clustering and Region Growing

R. Rizal Isnanto
Department of Computer Engineering
Diponegoro University
Semarang, Indonesia
email: rizal@ce.undip.ac.id

Oky Dwi Nurhayati
Department of Computer Engineering
Diponegoro University
Semarang, Indonesia
email: okydwi.n@gmail.com

Tyas Panorama Nan Cerah
Department of Computer Engineering
Diponegoro University
Semarang, Indonesia
email: panoramacerah@gmail.com

Abstract— The calculation of the area of mangrove forests by conventional methods requires much time and energy. In this study, a tool for calculating the area of mangrove forests in Southeast Sulawesi Province, Indonesia, using satellite imagery is developed on the basis of two segmentation methods, k-means clustering and region growing. We then compare those two methods to obtain the optimal method to calculate the area of mangrove forests. Before this research, there were no researchers who calculated the area of mangrove forests in Southeast Sulawesi using both methods. We constructed a calculation algorithm using Matlab, which includes different stages of digital image processing. The area of mangrove forests is calculated on the basis of the number of pixels with an area density of 900 m²/pixel. The accuracy of the two segmentation methods is compared for identical areas obtained by the National Institute of Aviation and Space in Indonesia (LAPAN), i.e., the area obtained by LAPAN is used as a reference in calculating the accuracy. The accuracy of the region growing segmentation method is 33.33%, whereas that by the k-means clustering segmentation method under optimum conditions is 59.26% in the application of 12 clusters.

Keywords— *mangrove forest, k-means clustering, region growing, satellite imagery, Southeast Sulawesi Province*

I. INTRODUCTION

Mangrove forests grow along tropical beaches or river mouths that are affected by tides. Indonesia is a country that has the largest area of mangrove forests in the world, which is equivalent to 23% of the world's mangrove ecosystem of a total area of 16530000 ha. However, such forests are damaged from year to year. This damage is caused by the conversion of mangrove forests into fishponds, settlements, or mining activities around the coast. In addition, mangrove forests are increasingly threatened owing to the extensive uncontrolled land uses derived from high community preferences to own land and settlements in coastal areas [1].

Satellite image processing has been widely used to identify and analyze changes in the shape, area, and other conditions of a location. One application of satellite image processing is the identification of the area of mangrove forests by image segmentation. The purpose of image segmentation is to segment or separate an image into homogeneous regions on the basis of certain similarity criteria, e.g., to separate the main object from its background.

Image segmentation is used to identify mangrove forests by dividing an image into homogeneous regions on the basis of certain similarity criteria, as in [2–5]. Two examples of algorithms used for segmentation are *k*-means clustering segmentation reported in [3] and [4] and region growing segmentation described in [5]. *k*-Means clustering

segmentation divides a number of objects into regions on the basis of existing categories by referring to the given midpoint, whereas region growing segmentation starts from pixel seeds and develops to form regions. The *k*-means clustering segmentation in [3] can eliminate image noise, whereas the region growing segmentation in [4] cannot reduce noise. Although the two methods have different characteristics, they have some similarities. One of the similarities is in determining a pixel to be a region or group, i.e., with one point as the center and forming a region with certain requirements or properties, i.e., the closest distance between pixels. However, these conventional segmentation methods cannot provide sufficiently accurate data to distinguish mangrove forests from non-mangrove forests. Thus, a new system that aims to assist the accurate calculation of the area of mangrove forests needs to be developed. In this research, we used Landsat-8 images of mangrove forests in Southeast Sulawesi Province, Indonesia, to examine the accuracy of the two segmentation methods [6-8].

The calculation of the area of mangrove forests in [7] and [8] is not based on image segmentation using *k*-means clustering nor region growing. In this study, we aim to implement and analyze the *k*-means clustering segmentation and region growing segmentation methods to calculate the area of mangrove forests by using Landsat-8 imagery on the basis of the number of pixels identified. The pixels are then considered as the area of the mangrove forests. The accuracy of the two methods was calculated by using reference data on the mangrove forest area from the National Institute of Aviation and Space in Indonesia (LAPAN) [9]. In this paper, we first describe the two methods for calculating the area of mangrove forests, namely, the *k*-means clustering color image segmentation and region growing segmentation methods. The method with the higher accuracy was determined.

Another research was conducted on the tsunami-affected areas in Aceh using satellite imagery by Solehatin and Melita, who developed a system for identifying tsunami affected areas by the region growing segmentation method [10]. This research provided information on the size of the area affected by the tsunami generated by an earthquake with a magnitude of 8.9 on the Richter scale.

Arief, Prayogo, and Hamzah explained that the segmentation process can be generally done using three approaches, i.e., segmentation based on the boundary approach using the thresholding method, based on the edge approach using mathematical gradient or Laplacian operators, and based on the region approach [11]. The segmentation algorithms adopted in this study are divided

into three stages: applying reduction operations between AVNIR-2 data bands, calculating region growing, and mangrove clustering. The calculated area of mangrove forests on Lancang Island was 17.24 ha. A comparison of the results with data obtained from Regional Control Agency for Environmental Impacts in Indonesia (BAPEDALDA) in 2000 shows that the method has an accuracy of 95.5%.

II. Materials and Methods

A. Landsat-8 Imagery

Landsat-8 is a remote sensing satellite that continuously provides high-quality infrared images of all regions of the Earth in real time [12]. Landsat-8 satellite image data have the highest spatial resolution of 15 m and the lowest spatial resolution of 100 m [6][12]. Spatial resolution is the size of the smallest object that can be distinguished from other objects. Satellite imagery has been widely used to map mangroves with different degrees of success. Landsat satellite with a resolution of 30 m provided the accurate mangrove maps [12].

Spatial resolution in satellite imagery determines the scale of the mapping produced, or vice versa. If a particular scale is desired, then an appropriate spatial resolution is required. High-resolution satellite imagery will produce more detailed information about mangroves. However, high-resolution imaging is relatively expensive, which is a limitation in research using satellite imaging. Ultimately, accurate mapping, no matter how scalable, is an essential factor that must be considered in acquiring mangrove information and proper processing. Landsat-8 imagery can not only identify mangroves and non-mangroves but also identify mangrove density. However, mangrove species identification has not been possible with Landsat-8 imagery.

B. Mangroves and satellite image processing

Image processing starts from image acquisition by Landsat-8 satellite. The images obtained are filtered and enhanced, which includes the merging of images obtained from different channels, then corrected in terms of radiometric and geometric measurements. Then, color composites are selected to identify mangrove forests, followed by cropping the resulting satellite images. The process continues with segmentation by k-means clustering or region growing on an RGB image. The next process is the representation and description of images, which involve the calculation of the area of the mangrove forests by the segmentation methods. Lastly, the calculated areas of mangrove forests are compared with reference data.

The following are the details of image processing to obtain the areas of mangrove forests.

(1) Image acquisition

The object of image acquisition in the form of a Landsat-8 satellite image can be downloaded for free and was obtained from the official website of United State Geological Survey (USGS) (https://earthexplorer.usgs.gov). The downloaded images from different channels (bands) have different characteristics because we can combine and display channels of information digitally using the three primary colors (i.e. red, green, and blue). The data from each channel is represented as a primary color and depending on the relative brightness (i.e., the digital value) of each pixel in each channel, the primary colors combine in different proportions to represent different colors. Images are then merged to obtain a complete satellite image to select color composites to identify the mangrove forest to be observed.

(2) Image enhancement

Image enhancement is the process of manipulating images so that the results are more representative of the object being observed. The initial image enhancement process is radiometric correction, which includes the correction of effects related to the increase in the image contrast, thus ensuring that the recorded object is easily interpreted or analyzed to produce correct data in accordance with field conditions [13].

Satellite imagery can also be processed by selecting the best channel combination using the optimum index factor (OIF). Compared with manual combination selection, the OIF makes it easy to select statistical composite combinations that are appropriate for identifying an object by quantitative assessments. OIF is statistically calculated for every possible combination of three channels for the image that provides the best RGB combination [8]. With these composites, a displayed RGB image will show mangrove forests in dark red, non-mangrove forests in bright red, shallow waters in deep blue, and deep sea in dark (black) [8].

(3) k-Means clustering

Clustering is a method to divide a set of data into a specific number of groups [15]. One of the popular methods is the k-means clustering, which divides a collection of data into k groups of data [16][17]. It classifies a given set of data into k disjointed clusters. The k-means algorithm consists of two phases. In the first phase, the centroid for k clusters is calculated, and in the second phase, k-means clustering takes each point in the cluster which has the nearest centroid from the respective data point. Different methods are used to define the distance of the nearest centroid. One of the methods is the use of the Euclidean distance. Once the grouping is completed, the new centroid of each cluster is recalculated. On the basis of this new centroid, a new Euclidean distance is calculated between each centroid and each data point. Each cluster in the partition is defined by its member objects and by its centroid. The centroid for each cluster is the point at which the sum of distances from all the objects in that cluster is minimized. Therefore, the k-means algorithm is an iterative algorithm that minimizes the sum of distances from each object to its cluster centroid over all clusters.

The clustering process starts by identifying the data to be clustered, c_{ij} $(i = 1, \ldots, n; j = 1, \ldots, m)$, where n is the number of data to be clustered and m is the number of variables. In the initial iteration, the center of each cluster is determined arbitrarily, c_{kj} $(k = 1, \ldots, k; j = 1, \ldots, m)$. Then, the distance between two data points is calculated against each cluster center. To calculate i-distance data c_i at the center of each k-th cluster (c_k), the distance expressed as d_{ik}, can be determined using the Euclidean equation as follows [3][18].

$$d_{ik} = \sqrt{\sum_{j=1}^{m}\left(c_{ij} - c_{kj}\right)^2} \qquad (1)$$

A data point is considered to be a member of the k-th cluster if its distance from the center of the k-th cluster is the smallest among other clusters. This distance can be calculated using Eq. (2). The data points are grouped into members in each cluster.

$$\min \sum_{k=1}^{k} d_{ik} = \sqrt{\sum_{j=1}^{m}\left(c_{ij} - c_{kj}\right)^2} \qquad (2)$$

The new cluster center value can be calculated by finding the average value of the data point that is a member of the cluster using Eq. (3) [3].

$$c_{kj} = \frac{\sum_{i=1}^{p} x_{ij}}{p}, \qquad (3)$$

Here x_{ij} is i-th data point to be clustered with variable j and p is number of members of the k-th cluster [3]

Although k-means clustering has the great advantage of being easy to implement, it has some drawbacks. The quality of the final clustering results depends on the selection of the initial centroid, which is arbitrary. Therefore, if the initial centroid is randomly selected, a different result will be obtained for different initial centers. For this reason, the initial center should be carefully chosen to acquire the desired segmentation. The other drawback is its long computational time during the k-means clustering. The computational time depends on the number of data points, the number of clusters, and the number of iterations [18].

(4) Region growing segmentation

In region growing segmentation, pixels or subregions are grouped into larger regions on the basis of predetermined criteria for growth. The basic approach is to start with several seed points. From a point, the area grows with the addition of neigh-boring pixel seeds that have the same properties, such as the specific range of gray or color levels, as those of the initial seed. Regional growth stops when no more pixels match the criteria for inclusion in the region. Criteria such as intensity, texture, and color are local properties and are not used in the calculation by the region growing method [17].

Kamdi and Krishna described the advantages and disadvantages of the region growing algorithm [19]. The advantages are as follows: this method (1) correctly separates the regions that have the same definition properties; (2) provides the original images that have clear edges and produces good segmentation results; (3) has a simple concept; (4) requires only a few seed points to represent the property and then grow the region; (5) enables multiple criteria to be simultaneously chosen; and (6) performs well with respect to noise. The dis-advantages include the long computational time, resulting in high power consumption and noise or variation of intensity that may result in holes or over-segmentation. In addition, the region growing method may not distinguish the shading of real images.

Wang, Song, and Jiang improved the image segmentation method based on three-dimensional region growing algorithm in medical applications. Their experimental results showed that their proposed method can effectively improve the accuracy of liver segmentation [20]. Erwin, Saparudin, Nevriyanto, and Purnamasari compared image segmentation algorithms, including the region growing method. They concluded that the grown region shows that the segmentation of the surrounding pixel (neighbor) remains inhomogeneous, thus ensuring that the object can be segmented from its background. Again, the region growing method involves a long computation process [21].

Synthu Preetha, Suresh, and Bosco suggested that automatic seeded region growing algorithm can be used to properly segment color images. On the basis of the application, regions of interest might have differed; hence, none of the segmentation algorithms were satisfactory for general applications. Image segmentation is a process of clustering pixels into salient image regions, i.e., regions corresponding to individual surfaces, objects, or natural parts

of objects. Image segmentation plays a vital role in image analysis and computer vision applications [22].

Erwin, Saparudin, Nevriyanto, and Purnamasari provided the theoretical basis and some stages of the region growing method. Region-based segmentation includes the connecting steps between pixels to choose whether these pixels belong to the same region or not. Mathematically, region-based segmentation method can be explained systematically to divide the image I into n, S_1, S_2, $\cdots$, S_n, to emphasize the following properties [21]:

1. $\cup_{x=1}^{n} S_x = I$,
   Where S_x is a connected region, $x = 1, 2, \ldots, n$,
2. $S_x \cap S_y = \emptyset$ for all x and $y, x \neq y$,
3. $P(S_x) = $ TRUE for $x = 1, 2, \ldots, n$,
4. $P(S_x \cup S_y) = $ FALSE for any adjacent regions S_x and S_y.

Here, n is the number of regions, $P(S_i)$ is a logical predicate obtaining the points in a set S_i, and $\emptyset$ is an empty set.

C. Research objects

The data used to identify mangrove forests were obtained by the Landsat-8 OLI/TIRS satellite in six districts (Bombana Regency, North Buton Regency, Kolaka Regency, Konawe Regency, South Konawe Regency, and Muna Regency), Southeast Sulawesi Province, Indonesia, in 2016. All images were obtained free of charge from the official website of USGS Earth Explorer (https://earthexplorer.usgs. gov/) [12]. The reference images used as comparisons were taken from the same region, Southeast Sulawesi from the official website of LAPAN (http:// spbn.pusfatja.lapan.go.id [9]) also in the 2016 period. Fig. 1 shows the distribution of mangrove forests in Indonesia, with the area of Southeast Sulawesi is encircled [23]. Fig. 2 shows some photos of mangrove forests in Southeast Sulawesi.

D. System Requirements Analysis

We used the Windows 7 32-bit operating system, Matlab version R2015a, and Er-Mapper version 7.0 on a Compaq Laptop with a 2.3 GHz AMD Athlon II Dual Core P360 processor with 2 GB of 1333 MHz DDR3 memory. The satellite data were obtained by choosing channel combinations 5, 6, and 3 that were determined to identify mangrove forest objects. Clear satellite data objects were then corrected radiometrically and geometrically. The 27 input JPEG images had sizes ranging from 109 ×113 pixels to 505 × 519 pixels.

E. System Design

Fig. 3(a) shows the flowchart of k-means clustering segmentation, and Fig. 3(b) shows the flowchart of the region growing segmentation. The two segmentation methods described in Figs. 3(a) and 3(b) are then compared to obtain the optimal method to calculate the area of mangrove forests. Fig. 4 shows the flowchart of a mangrove forest area identification system designed using satellite imagery.

III. RESULTS AND DISCUSSIONS

Before image processing, six steps of processing satellite images are performed: (1) merging of satellite image channels, (2) radiometric correction, (3) geometric correction, (4) selection of channel combinations, (5) merging of satellite images, and (6) cropping of images on the mangrove object [13]. Satellite imagery is then processed

using the algorithm described above so that the area of the mangrove forests can be calculated. Image segmentation applied in this algorithm is *k*-means clustering or region growing. The results of the two methods are then compared to obtain the optimal identification results. The area of mangrove forests can be calculated by multiplying the number of pixels of the mangrove object image by 30×30 m^2 of the Landsat-8 satellite images (1 pixel represents an area of $30 \times 30 = 900$ m^2), which is the spatial resolution of Landsat-8 imagery used in this study [7].

Fig. 1. Distribution of mangrove forests in Indonesia, with the area of Southeast Sulawesi encircled.

Fig. 2. Photos of mangrove forests in Southeast Sulawesi Province.

A. *k*-Means Clustering Segmentation

k-Means clustering segmentation is used to label each cluster on the basis of the number of clusters selected by the user. When selecting *k*-means clustering segmentation on the computer screen, users will be asked to enter the number of clusters or groups to be used to label images according to the number of selected clusters. The number of clusters provided in the pop-up menu starts from 2 to 20 clusters. The number of clusters is determined manually so that users can distinguish between cluster values.

The segmentation process is performed by grouping images into clusters randomly on the basis of histograms and then determining the distance of a pixel to the centroid (cluster midpoint). Then, the minimum distance between pixels and the centroid is determined, ensuring that groups are formed on the basis of the minimum value of pixels with respect to the centroid. From these groups, the mean of each member from one cluster is calculated. From the average value of each cluster, we can obtain a new centroid value, with which the process is repeated iteratively. The segmentation process stops when the average value of the cluster members remains the same.

As a result of the segmentation process, images were grouped according to the number of clusters entered in the algorithm by the user. The next stage, namely, calculating the area of mangrove forests, is based on the results of the above segmentation of the location of mangrove forests. Mangrove forests are determined with the object closure technique, which only displays the desired object (masking) using the thresholding method in the hue, saturation, value (brightness)

(HSV) color space as a reference. This thresholding method is performed by determining the minimum and maximum values of each channel in the HSV color space. Then, from predetermined minimum and maximum values, a cluster image that matches the values from the previous segmentation image is output.
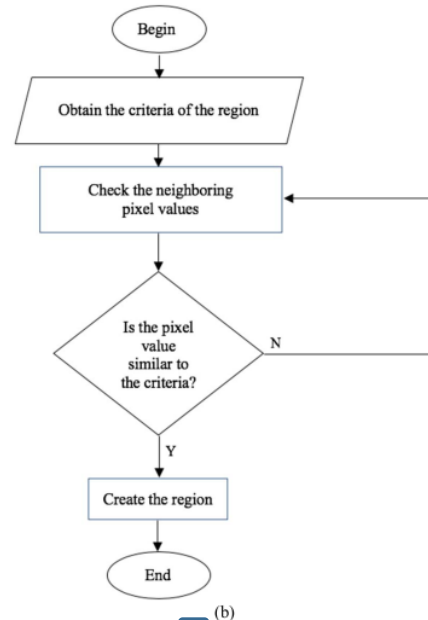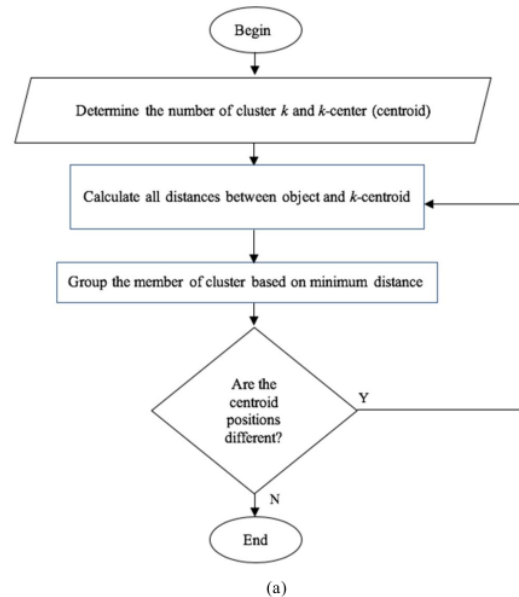

(a)

(b)

Fig. 3 Flowcharts of (a) *k*-means clustering segmentation and (b) region growing segmentation.

The final result of the mangrove forests has the same color as the result of *k*-means clustering segmentation in the previous process. However, in our study, non-mangrove forests are displayed on a gray level to distinguish them from mangrove forests. Fig. 5 shows the example of results of the segmentation process using 11 and 20 clusters and followed by masking the non-mangrove forests into gray-level pixels.
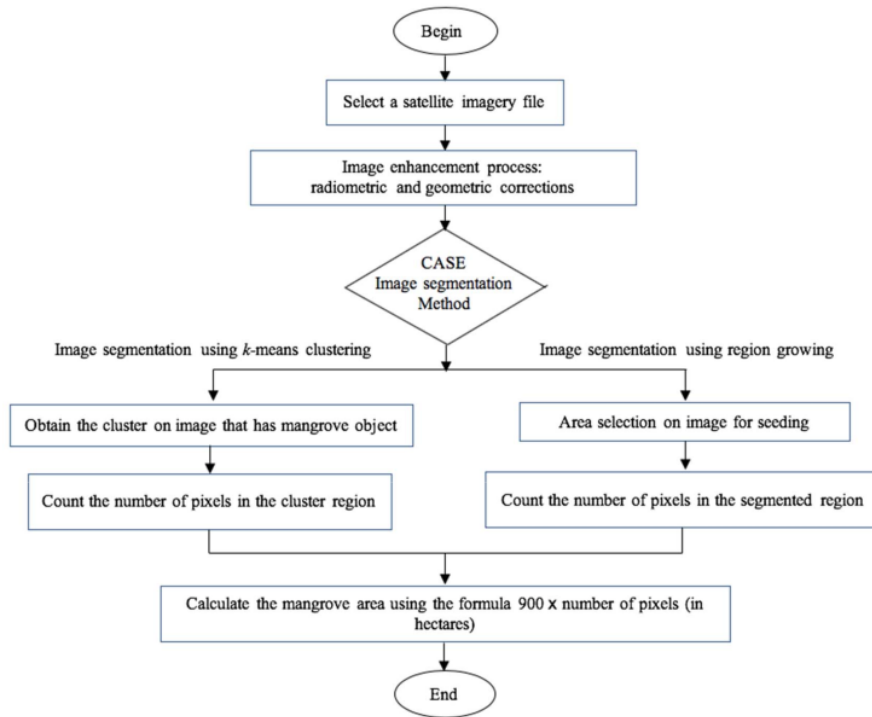
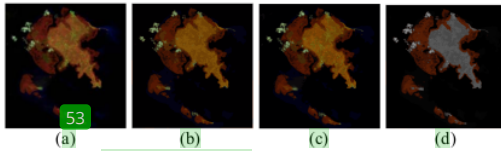Fig. 4. Flowchart of system for calculating area of mangrove forests.

(a)   (b)   (c)   (d)

Fig. 5. Results of k-means clustering to segment the mangrove object from satellite imagery.(a) Original satellite image; (b) segmentation using 11 clusters; (c) segmentation using 20 clusters; and (d) masking non-mangrove objects into gray level pixels.

B. Region Growing Segmentation

The first process of region growing segmentation is the determination of the gray level value to be used as a seed value. This step ensures that the seed value and the threshold value can be assigned automatically to more than one satellite image. Histograms are compared among satellite images in order to find similarities. We found similarities starting from intensity 0, which has a relatively large number of pixels. As the intensity value increases, the number of pixels decreases and the decrease stops at an intensity value of approximately 10, and the number of pixels is relatively stable until the intensity value is approximately 35.

In some tests, the mangrove intensity values were more than 35. To overcome this problem, we adjusted the intensity values from 45 to 55 to become 35 so that the seed value used is 35, and the threshold value used is 10 to determine the intensity limit. From the region growing segmentation results, the intensity value is changed to make the value of the segmentation result 1 if it has an intensity value of more than 10 and a value of 0 if the intensity value is less than 1.

From the determined seed and threshold values, the image segmentation results are in the form of binary images with mangrove areas having a value of 1 and non-mangrove areas having a value of 0. From the image of segmentation results, the initial image is merged with the segmented image to obtain a clear image of mangrove and non- mangrove objects. Fig. 6 shows the final segmentation result obtained using the region growing method.

C. Mangrove Forest Area Calculation Process

This process involves counting the number of pixels of segmented images and calculating the area of the number of pixels that have been obtained. The number of areas calculated using the sum command to add the value of 1 in a segmented image, where the image value of 1 is an image that has a mangrove object.

The areas of the same location are compared with the data of the same year taken from the LAPAN website [9]. In k-means clustering segmentation, data on clusters 11, 12, and 13 were included because the data of these clusters are similar to those obtained from the LAPAN website.
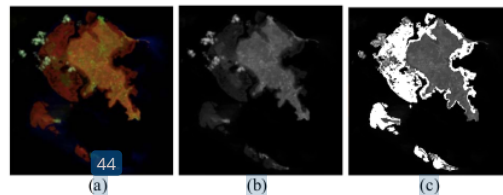

(a)   (b)   (c)

Fig. 6. Results of region growing method to segment the mangrove object from satellite imagery: (a) Original satellite image; (b) after converting into a grayscale image; and (c) segmentation using region growing method.

The algorithm used in this method includes the unsupervised learning method, which groups pixels into several groups only on the basis of certain calculations without training and is used as a reference for classification. Table 1 shows the calculation results obtained by *k*-means clustering segmentation. Table 2 shows the calculation results obtained by region growing segmentation.

D. Accuracy of Research Results

The accuracy of the results of this study is based on the accuracy of the individual observation in each image and the overall data accuracy of both segmentation methods. Equation (4) is used to calculate the accuracy for individual observation. Equation (5) is used to calculate the average accuracy in the research. Number of correct classifications show the percentage of classifications that have individual accuracy more than 80% of the total classification observations conducted.

Accuracy of individual observation

$$= \left(1 - \left(\left|\frac{\text{calculated area} - \text{reference area}}{\text{reference area}}\right|\right)\right) \times 100\% \quad (4)$$

$$\text{Overall accuracy} = \frac{\text{number of correct classification}}{\text{number of total observations}} \times 100\% \quad (5)$$

Table 3 shows the comparison of accuracies between the *k*-means clustering and the region growing calculated using Eqs. (4) and (5). Fig. 7 shows the accuracies of *k*-means clustering with three numbers of clusters (11, 12, and 13) and region growing. Table 3 shows that the calculation using the *k*-means clustering method has the highest accuracy of 59.26% in the application of 12 clusters. The region growing segmentation obtained an accuracy of 33.33%. Thus, *k*-means clustering has a higher average accuracy than region growing in calculating the area of mangrove forests.
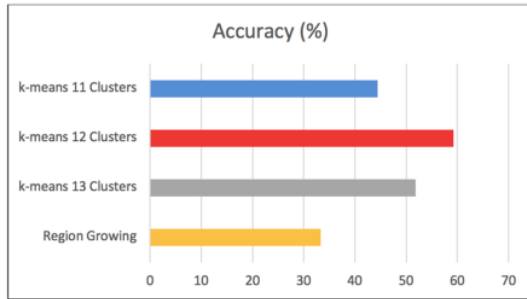

Fig. 7. Bar charts of accuracies of the methods: *k*-means clustering with three alternatives of clusters (11, 12, and 13) and region growing segmentation

The low level of accuracy may be due to the assumptions used in determining the correct classification. In this research, the number of correct classification shows the percentage of classifications that have individual accuracy more than 80%

of the total classification observations conducted. With this assumption, lowering the individual accuracy rate will increase the level of accuracy. Conversely, if the individual accuracy number is increased, it will automatically decrease the level of accuracy.

K-means clustering which has a higher average accuracy in this case rather than region growing segmentation does not indicate that *k*-means clustering is better than region growing segmentation. *K*-means clustering and region growing segmentations have their own suitability in specified cases. Mustafa and Hassan compare 6 (six) methods to segment the medical images, including *k*-means and region growing segmentations. They provided their study result that region growing shows the best method or algorithm that gives better segmentation with physical and structural similarity [24]. While, Said and Ibrahim conducted a comparative study of segmentation techniques for detection of tumors based on MRI brain images. They study 4 (four) methods, including *k*-means clustering and region growing. They concluded that *k*-means method is the best segmentation method among the other four segmentation methods which implemented [25].

E. Limitations of the Research and Future Works

1. The accuracy of each segmentation method is still far from 100% owing to the differences in satellite data in this research from the data on the LAPAN website used for comparison. Subsequent studies are expected to achieve higher accuracies.
2. The input image is obtained by Landsat-8 satellite, which has a resolution of 30 m and can only detect mangrove and non-mangrove areas. In future research, other satellites that have higher resolution should be used, such as the Quickbird satellite, GeoEye, and IKONOS, to ensure that the mangrove density in an area can also be determined.
3. The algorithms provide means of mangrove forest identification only by using *k*-means clustering segmentation and region growing segmentation. In future research, it is expected to use other methods, such as the global thresholding, multi-thresholding, parametric deformable model, morphological-based segmentation, and fuzzy *c*-means clustering.

IV. CONCLUSIONS

The following conclusions were obtained from this research. A system of calculating the area of mangrove forests is implemented by using two segmentation methods: *k*-means clustering image segmentation and region growing image segmentation. We obtained an accuracy of 59.26% by *k*-means clustering segmentation, whereas an accuracy of 33.33% was obtained by region growing segmentation.

TABLE I. CALCULATION RESULTS ON SATELLITE IMAGES USING *k*-MEANS CLUSTERING SEGMENTATION

No	Region of mangrove forest	Cluster number						Reference area (ha)
		11		12		13		
		Pixel number	Calculated area (ha)	Pixel number	Calculated area (ha)	Pixel number	Calculated area (ha)	
1	Kabaena Island 1	2,218	199.620	2,148	193.320	1,829	164.610	168
2	Kabaena Island 2	6,823	614.070	6,841	615.690	8,186	736.740	716.56
3	Kolaka	-	-	2,452	220.680	2,261	203.490	266.65

No	Region of mangrove forest	Cluster number						Reference area (ha)
		11		12		13		
		Pixel number	Calculated area (ha)	Pixel number	Calculated area (ha)	Pixel number	Calculated area (ha)	
4	Konawe 1	-	-	-	-	-	-	526.02
5	Konawe 2	1,451	130.590	2,387	214.830	1,444	129.960	1,185.77
6	Konawe 3	7,385	664.650	7,351	661.590	7,331	659.790	1,313
7	Konawe 4	8,907	801.630	8,765	788.850	5,860	527.400	1,448
8	Konawe 5	-	-	7,197	647.730	7,125	641.250	814.34
9	Konawe 6	48,743	4,386.870	49,398	4,445.820	48,294	4,346.460	5,803.83
10	Konawe 7	6,314	568.260	6,249	562.410	9,459	851.310	557
11	Muna 1	3,769	339.210	3,304	297,360	3,214	289,260	257
12	Muna 2	2,078	187.020	1,950	175,500	1,888	169,920	236
13	Muna 3	3,141	282.690	3,136	282,240	3,064	275,760	317
14	Muna 4	6,195	557.550	8,911	801,990	8,834	795,060	846
15	Muna 5	5,508	495.720	5,506	495,540	5,465	491,850	471
16	Muna 6	1,475	132.750	1,422	127,980	2,276	204,840	208.51
17	Muna 7	1,852	166.680	2,747	247,230	2,729	245,610	251.26
18	Muna 8	12,056	1,085.040	12,005	1,080.450	11,914	1.072,260	1,205.85
19	Muna 9	14,328	1,289.520	16,085	1,447.650	15,962	1,436.580	1,350.77
20	North Buton 1	1,650	148.500	1,784	160.560	1,776	159.840	819
21	North Buton 2	22,774	2,049.660	38,502	3,465.180	28,279	2,545.110	5,687
22	North Buton 3	36,957	3,326.130	31,897	2,870.730	32,526	2,927.340	3,604.19
23	North Buton 4	10,989	989.010	10,903	981.270	6,882	619.380	1,053
24	North Buton 5	14,380	1,294.200	13,503	1,215.270	12,657	1,139.130	1,279
25	North Buton 6	9,247	832.230	14,906	1,341.540	14,749	1,327.410	1,213
26	North Buton 7	10,348	931.320	10,150	913.500	9,802	882.180	1,039.15
27	North Buton 8	4,347	391.230	4,334	390.060	3,612	325.080	450

TABLE II. CALCULATION RESULTS ON SATELLITE IMAGES USING REGION GROWING SEGMENTATION

No	Region of mangrove forest	Pixel number	Calculated mangrove area (ha)	Reference area (ha)
1	Kabaena Island 1	185	16.65	168
2	Kabaena Island 2	8,210	738.9	716.56
3	Kolaka	2,678	241.02	266.65
4	Konawe 1	3,830	344.7	526.02
5	Konawe 2	1,910	171.9	1,185.77
6	Konawe 3	9,940	894.6	1,313
7	Konawe 4	11,954	1,075.86	1,448
8	Konawe 5	15,407	1,386.63	814.34
9	Konawe 6	49,245	4,432.05	5,803.83
10	Konawe 7	10,315	928.35	557
11	Muna 1	2,726	245.34	257
12	Muna 2	2,412	217.08	236
13	Muna 3	2,755	247.95	317
14	Muna 4	7,095	638.55	846
15	Muna 5	4,613	415.17	471
16	Muna 6	2,950	265.5	208.51
17	Muna 7	2,789	251.01	251.26
18	Muna 8	10,798	971.82	1,205.85
19	Muna 9	14,049	1,264.41	1,350.77
20	North Buton 1	2,663	239.67	819
21	North Buton 2	24,264	2,183.76	5,687
22	North Buton 3	36,657	3,299.13	3,604.19
23	North Buton 4	8,305	747.45	1,053
24	North Buton 5	11,028	992.52	1,279
25	North Buton 6	2,699	242.91	1,213
26	North Buton 7	8,860	797.4	1,039.15
27	North Buton 8	3,820	343.8	450

TABLE III. COMPARISON OF ACCURACIES OF k-MEANS CLUSTERING AND REGION GROWING SEGMENTATION

No	Region of mangrove forest	Accuracy of k-means clustering segmentation for each cluster (%)			Accuracy of region growing segmentation (%)
		11	12	13	
1	Kabaena Island 1	81.18	84.93	97.98	9.91
2	Kabaena Island 2	85.70	85.92	97.18	96.88
3	Kolaka	0.00	82.76	76.31	90.39
4	Konawe 1	0.00	0.00	0.00	65.53
5	Konawe 2	11.01	18.12	10.96	14.50
6	Konawe 3	50.62	50.39	50.25	68.13
7	Konawe 4	55.36	54.48	36.42	74.30
8	Konawe 5	0.00	79.54	78.74	29.72
9	Konawe 6	75.59	76.60	74.89	76.36

10	Konawe 7	97.98	99.03	47.16	33.33
11	Muna 1	68.01	84.30	87.45	95.46
12	Muna 2	79.25	74.36	72.00	91.98
13	Muna 3	89.18	89.03	86.99	78.22
14	Muna 4	65.90	94.80	93.98	75.48
15	Muna 5	94.75	94.79	95.57	88.15
16	Muna 6	63.67	61.38	98.24	72.67
17	Muna 7	66.34	98.40	97.75	99.90
18	Muna 8	89.98	89.60	88.92	80.59
19	Muna 9	95.47	92.83	93.65	93.61
20	North Buton 1	18.13	19.60	19.52	29.26
21	North Buton 2	36.04	60.93	44.75	38.40
22	North Buton 3	92.29	79.65	81.22	91.54
23	North Buton 4	93.92	93.19	58.82	70.98
24	North Buton 5	98.81	95.02	89.06	77.60
25	North Buton 6	68.61	89.40	90.57	20.03
26	North Buton 7	89.62	87.91	84.89	76.74
27	North Buton 8	86.94	86.68	72.24	76.40
	Overall accuracy (%)	**44.44**	**59.26**	**51.85**	**33.33**

REFERENCES

[1] M. Vitasari, "Kerentanan Ekosistem Mangrove Terhadap Ancaman Gelombang Ekstrim/Abrasi di Kawasan Konservasi Pulau Dua Banten," *Bioedukasi: Jurnal Pendidikan Biologi*, vol. 8, no. 2, pp. 33-36, 2015.

[2] Pusat Pemanfaatan Pengindraan Jauh, *Pedoman Teknik Pengolahan Data Pengindraan Jauh Landsat-8 untuk Mangrove.* Lembaga Penerbangan dan Antariksa Nasional, 2015.

[3] E.T. Opa, "Analisis Perubahan Lahan Mangrove di Kabupaten Pohuwato Propinsi Gorontalo dengan Menggunakan Citra Landsat," *Jurnal Perikanan dan Kelautan Tropis*, vol. 6, no. 2, pp. 79-82, 2010.

[4] A.K.S. Manoppo, N. Anggraini, and Y. Marini, "Identifikasi Mangrove dengan Meto-de Optimum Index Factor (OIF) pada Data SPOT6 dan Landsat8 di Pulau Lingayan," in *Pertemuan Ilmiah Tahunan XX dan Kongres VI MAPIN: Masyarakat Ahli Penginderaan Jauh*, Bogor, Indonesia, Feb. 2015.

[5] K.T. Setiawan, N. Aggraini, and A.K.S. Manoppo, "Estimasi Perhitungan Luas Daerah di Pulau-pulau Kecil Menggunakan Data Citra Satelit Landsat-8 Studi Kasus: Pulau Pramuka Kepulauan Seribu DKI Jakarta," in *Seminar Nasional Pengindraan Jauh*, Indonesia, 2016, pp. 294-300.

[6] A.I. Kesuma, Herman, Munawir, *Penerapan Metode Klaster K-Means pada Segmentasi Warna Citra Digital dengan Pemrograman R*, Fakultas Ilmu Komputer, Universitas Sumatera Utara, Medan, ISSN: 2548-4540, 2016.

[7] A. Atina, "Segmentasi Citra Paru Menggunakan Metode K-Means Clustering," *Jurnal Pendidikan Fisika dan Keilmuan*, vol. 3, no. 2, 2017, pp. 55-65.

[8] F. Kanditami, D. Saepudin, and A. Rizal, "Analisis Contrast Limited Adaptive Histogram Equalization (CLAHE) dan Region Growing dalam Deteksi Gejala Kanker Payudara pada Citra Mammogram," *Jurnal Elektro Unika Atma Jaya*, vol. 7, no. 1, 2014, pp. 15-28.

[9] Pusat Pemanfaatan Penginderaan Jauh LAPAN, "Sebaran Perubahan Hutan Mangrove Indonesia tahun 2016," October 2017. [online]. Available: http://spbn.pusfatja.lapan.go.id/layers/geonode.

[10] S. Solehatin, and Y. Melita, "Identifikasi Luas Bencana Tsunami dengan Menggunakan Segmentasi Citra pada Metode Seed Region Growing," *Jurnal Informatika dan Komputer*, 2(1), 2012, pp. 25-31.

[11] M. Arief, T. Prayogo, and R. Hamzah, "Automatic of Segmentation Method for Extraction Mangrove Forest by Using Avnir-2 Satellite Data Case Study: Lancang Island." *Jurnal Teknologi Dirgantara*, Vol. 11 No. 1 Juni 2013, pp. 35-48

[12] Department of the Interior U.S. Geological Survey, "Landsat-8 (L8) Data Users Handbook," U.S. Geological Survey, LSDS-1574 Version 2.0, 2016.

[13] Supriatna, W., Sukartono, "Teknik Perbaikan Data Digital (Koreksi dan Penajaman) Citra Satelit," Buletin Teknik Pertanian, (7): 1, 2002.

[14] A. Nontji, "Laut Nusantara," Djambatan, Jakarta, 2015.

[15] N. Dhanachandra, K. Manglem, and Y.J. Chanu, "Image Segmentation using K-means Clustering Algorithm and Subtractive Clustering Algorithm," Procedia Computer Science 54 of The Eleventh International Multi-Conference on Information Processing-2015 (IMCIP-2015), doi: 10.1016/j.procs.2015.06. 090, 2015, pp. 764-771.

[16] S.S. Khan and A. Ahmad, "Cluster Centre Initialization Algorithm for K-means Cluster," Pat-tern Recognition Letters, 2004, pp. 1293–1302.

[17] S. Israil, "An Overview of Clustering Methods," In with: Application to Bioinformatics, 2013, pp. 101-110.

[18] A.S. Abdul-Nasir, M.Y. Mashor, and Z. Mohamed, "Colour Image Segmentation Approach for Detection of Malaria Parasiter using Various Colour Models and k-Means Clustering," WSEAS Transaction on Biology and Biomedecine, vol. 10, January 2013, pp. 41-55.

[19] K. Kamdi, and R.K. Krishna, "Image Segmentation and Region Growing Algorithm," International Journal of Computer Technology and Electronics Engineering (IJCTEE), vol. 2, no. 1, ISSN 2249-6343, 2012, pp. 103-107.

[20] Q. Wang, X. Song, and Z. Jiang, "An Improved Image Segmentation Method Using Three-dimensional Region Growing Algorithm," International Conference on Information Science and Computer Applications (ISCA 2013), 2013.

[21] E. Erwin, S. Saparudin, A. Nevriyanto, and D. Purnamasari, "Performance Analysis of Comparison between Region Growing, Adaptive Threshold and Watershed Methods for Image Segmentation," Proceedings of the International MultiConference of Engineers and Computer Scientists 2018, Vol I IMECS 2018, March 14-16, Hong Kong, 2018.

[22] M.M. Synthuja, J. Preetha, L.P. Suresh, and M.J. Bosco, "Image segmentation using seeded region growing," 2012 International Conference on Computing, Electronics and Electrical Technologies (ICCEET), Kumaracoil, 2012, pp. 576-583.

[23] A.W. Radiastuti, D.M. Yuwono, N. Niendyawati, G.H. Pramono, and B.D. Rahmanto, "Overview of National Thematic Data Integration (An Experience on One Map Mangrove Sulawesi)", Proceedings of 2nd International Conference of Indonesian Society for Remote Sensing (ICOIRS) 2016, doi: 10.1088/1755-1315/47/012012, pp. 1-15.

[24] I.D. Mustafa and M.A. Hassan, "A Comparison between Different Segmentation Techniques used in Medical Imaging", *American Journal of Biomedical Engineering*, vol. 6, no. 2, 2016, doi: 10.5923/j.ajbe.20160602.03, pp. 59-69.

[25] A.M. Said and F.S. Ibrahim. "Comparative Study of Segmentation Techniques for Detection of Tumors based on MRI Brain Images", *Journal of Bioscience, Biochemistry, and Bioinformatics*, vo. 8, no. 1, January 2018, doi: 10.1.17706/ijbbb.2018.8.1.1-10, pp. 1-10.

Area of Mangrove Forests Calculated by Color Image Segmentation Using k-Means Clustering and Region Growing

disease diagnosis by an unsupervised deep learning technology", Neurocomputing, 2019
Publication

14 en.wikipedia.org
Internet Source
<1%

15 Dongbin Chen. "chapter 13 Image Segmentation", IGI Global, 2008
Publication
<1%

16 Muhamad Brilliant, Suhendro Yusuf Irianto, Sri Karnila, R.Z. Abdul Aziz. "Land Cover Changes Detection Using Region Growing Segmentation", Journal of Physics: Conference Series, 2020
Publication
<1%

17 Submitted to Syiah Kuala University
Student Paper
<1%

18 Rusdiansyah Rusdiansyah, Harun Al Rasyid, Suryanto Sosrowidigdo. "Implementation of address recording management using the K-Means clustering classification algorithm in Kebayoran District, DKI Jakarta", SinkrOn, 2021
Publication
<1%

19 Submitted to Universitas Andalas
Student Paper
<1%

20 Ashraf M. Said, Fatma S. Ibrahim. "Comparative Study of Segmentation
<1%

Techniques for Detection of Tumors Based on MRI Brain Images", International Journal of Bioscience, Biochemistry and Bioinformatics, 2018
Publication

21 Submitted to Curtin University of Technology <1 %
Student Paper

22 E COX. "Fuzzy Clustering", Fuzzy Modeling and Genetic Algorithms for Data Mining and Exploration, 2005 <1 %
Publication

23 Nima Karimi, Kelvin Tsun Wai Ng, Amy Richter, Jason Williams, Hussameldin Ibrahim. "Thermal heterogeneity in the proximity of municipal solid waste landfills on forest and agricultural lands", Journal of Environmental Management, 2021 <1 %
Publication

24 Submitted to Pacific University <1 %
Student Paper

25 link.springer.com <1 %
Internet Source

26 utpedia.utp.edu.my <1 %
Internet Source

27 www.mdpi.com <1 %
Internet Source

28	laptop-review.jigsy.com Internet Source	<1 %
29	pdffox.com Internet Source	<1 %
30	repository.smuc.edu.et Internet Source	<1 %
31	repository.tudelft.nl Internet Source	<1 %
32	www.scientific.net Internet Source	<1 %
33	dspace.lboro.ac.uk Internet Source	<1 %
34	Abderrahmane ELBALAOUI, M.FAKIR -, N.IDRISSI -, A.MARBOHA -. "Review of Color Image Segmentation", International Journal of Advanced Computer Science and Applications, 2013 Publication	<1 %
35	Fathan Mustaghfirin, Erwin, Hadrians Kesuma Putra, Umi Yanti, Rahma Ricadonna. "The Comparison of Iris Detection Using Histogram Equalization and Adaptive Histogram Equalization Methods", Journal of Physics: Conference Series, 2019 Publication	<1 %

36 Majid Bagheri, Ali Akbari, Sayed Ahmad Mirbagheri. "Advanced control of membrane fouling in filtration systems using artificial intelligence and machine learning techniques: A critical review", Process Safety and Environmental Protection, 2019
Publication   <1%

37 Yangyang Guo, Dongjian He, Huaibo Song. "Region detection of lesion area of knee based on colour edge detection and bilateral projection", Biosystems Engineering, 2018
Publication   <1%

38 article.sapub.org
Internet Source   <1%

39 ejournals.umma.ac.id
Internet Source   <1%

40 eudl.eu
Internet Source   <1%

41 scholarworks.gsu.edu
Internet Source   <1%

42 Submitted to Durban University of Technology
Student Paper   <1%

43 Lim, Mikhiel, and Ilker Hacihaliloglu. "Segmentation of knee MRI using structure enhanced local phase filtering", Medical

Imaging 2016 Computer-Aided Diagnosis, 2016.

Publication

44	**de.scribd.com** Internet Source	**<1** %
45	**dias.library.tuc.gr** Internet Source	**<1** %
46	**documents.mx** Internet Source	**<1** %
47	**hdl.handle.net** Internet Source	**<1** %
48	**irdindia.in** Internet Source	**<1** %
49	**onlinelibrary.wiley.com** Internet Source	**<1** %
50	**worldwidescience.org** Internet Source	**<1** %
51	**www.engineeringletters.com** Internet Source	**<1** %
52	**www.jrrset.com** Internet Source	**<1** %
53	**www.meteo.be** Internet Source	**<1** %
54	**sjdgge.ppj.unp.ac.id** Internet Source	**<1** %

55   Akio Kimura, Tomoyuki Matsuzaka, Yukio Kagawa. "FIR-type and IIR-type neural networks, and their application to shape optimization of a magnetic pole", Inverse Problems in Science and Engineering, 2005
Publication   <1 %

56   Amir B. Geva. "Hierarchical-fuzzy clustering of temporal-patterns and its application for time-series prediction", Pattern Recognition Letters, 1999
Publication   <1 %

57   Emna Ben ‑ Abdallah, Khouloud Boukadi, Jaime Lloret, Mohamed Hammami. "CROSA: Context ‑ aware cloud service ranking approach using online reviews based on sentiment analysis", Concurrency and Computation: Practice and Experience, 2019
Publication   <1 %

58   Enquhone Alehegn. "Ethiopian maize diseases recognition and classification using support vector machine", International Journal of Computational Vision and Robotics, 2019
Publication   <1 %

Exclude quotes   Off   Exclude matches   Off
Exclude bibliography   On

Area of Mangrove Forests Calculated by Color Image Segmentation Using k-Means Clustering and Region Growing

FINAL GRADE

/0

GENERAL COMMENTS

Instructor